PCCP

PAPER

View Article Online
View Journal

Cite this: DOI: 10.1039/c5cp05236j

Fluorescence from an H-aggregated naphthalenediimide based peptide: photophysical and computational investigation of this rare phenomenon†

Shibaji Basak,[a] Nibedita Nandi,[a] Kalishankar Bhattacharyya,[b] Ayan Datta*[b] and Arindam Banerjee*[a]

Received 2nd September 2015,
Accepted 9th October 2015

DOI: 10.1039/c5cp05236j

www.rsc.org/pccp

Fluorescence associated with J-aggregated naphthalenediimides (NDIs) is common. However, in this study an NDI based synthetic peptide molecule is found to form a fluorescent H-aggregate in a chloroform ($CHCl_3$)–methylcyclohexane (MCH) mixture. An attempt has been made to explain the unusual fluorescence property of this H-aggregated NDI derivative. Time correlated single photon counting (TCSPC) shows that the average lifetime of the NDI based molecule is on the order of a few nanoseconds. It is revealed from the computational study that the transition from the second exited state (S_2) to the ground energy state (S_0) is responsible for the fluorescence as S_1 is a dark state. Such rare violation of Kasha's rule accounts for the unusual fluorescence properties of this type of NDI molecule in the H-aggregated state.

Introduction

Organic supramolecular materials[1] belong to a highly expanding area of current research in organic electronics and other related fields. The self-assembly of the organic semiconducting molecules leads to the formation of different types of functional aggregates and they have various applications in photovoltaics, field-effect transistors and others.[2] Covalent conjugates of amino acid and peptide based small fragments of organic semiconducting species are a rapidly growing area of current research.[3] This is because these molecules can be self-assembled by using various non-covalent interactions including hydrogen bonding, π–π, hydrophobic and electrostatic interactions, and others. Among these organic semiconductors, NDIs are an important class of n-type semiconducting molecules due to their molecular planarity, distinctive redox behavior and the π-acidity for making various supramolecular architectures.[4] The use of NDI-based molecules for photonic purposes is restricted owing to their lower quantum yield of fluorescence than that of their counterparts including perylene and other rylene dyes.[5] By regulating the aggregation behavior of NDI based molecules, a few attempts have been made to augment the fluorescence of NDI based molecules.[6] Another way to increase the fluorescence potentially is by substituting the NDI core.[7] In NDI based molecules, fluorescence can arise due to various factors including excimer emission, aggregation induced fluorescence and others in core un-substituted NDIs.

Moreover, several efforts have been directed to explore the type of aggregate (H- and/or J-type) that is formed by the self-assembly of various fluorescent dyes. This type of aggregate formation is reflected by the corresponding absorption spectrum of the aggregate and also by the blue or red shift of its absorption band compared to its monomeric species.[8] Many J-aggregates show fluorescence with high quantum yields,[9] in contrast to H-aggregates which are reported to be non-fluorescent.[8] Thus, the non-emissive character in the excited state of dye molecules is accepted as a general feature for H-aggregates. The non-emissive nature of H-aggregates can be understood from the dipole forbidden $S_1 \rightarrow S_0$ lowest energy transition (Kasha's rule).[10] Though there are only a few examples of fluorescent H-aggregates arising from the stacking of various dye molecules, the evidence coming from the fluorescent H-aggregated species of rylene dyes (NDIs, PDIs and others) is very rare.[11] In the course of our investigation on the self-association of NDI conjugated peptide/amino acid based derivatives,[4b,6c,d] a dipeptide based NDI molecule **1** was synthesized, purified, characterized and its self-association in different solvent systems was studied. Interestingly, molecule **1** forms an H-aggregated species[11] in $CHCl_3$–MCH solvent mixtures. Moreover, in the H-aggregated state peptide **1** exhibits a remarkable bluish white fluorescence and this phenomenon is very unusual, in contrast to the previously reported results for NDI based non-fluorescent H-aggregated species.

[a] Department of Biological Chemistry, Indian Association for the Cultivation of Science, Jadavpur, Kolkata – 700 032, India. E-mail: bcab@iacs.res.in
[b] Department of Spectroscopy, Indian Association for the Cultivation of Science, Jadavpur, Kolkata – 700 032, India. E-mail: spad@iacs.res.in

† Electronic supplementary information (ESI) available. See DOI: 10.1039/c5cp05236j

Computational studies made an attempt to explain this unusual behavior of H-aggregated NDI based peptide molecules.

Results and discussion

The synthesis and characterization of peptide **1** have been mentioned in the ESI.† The NDI conjugated peptide **1** (Fig. 1) is very soluble in $CHCl_3$. It remains in the monomeric state and produces a clear solution in this solvent. On the other hand, the molecule is sparingly soluble in MCH and it promotes the aggregation of these NDI molecules. So, the self-assembly of peptide **1** was first tested by dissolving it in $CHCl_3$ and then MCH was added to it gradually. Slow and gradual addition of MCH changes the aggregation pattern and it starts to form an opaque solution at the solvent composition 50 : 50 ($CHCl_3$: MCH). In pure $CHCl_3$ the monomeric solution of peptide **1** exhibits weak fluorescence. The further addition of MCH to the above mentioned solvent composition causes a transformation from monomeric feebly fluorescent (in $CHCl_3$) to the bluish white aggregate (Fig. 1) at the solvent composition 10 : 90 ($CHCl_3$: MCH) under exposure to a UV lamp (365 nm).

A solvent dependent UV-vis spectroscopic study of peptide **1** was performed to explore the aggregation pattern from the monomeric chromophore to the aggregated state by varying the composition of $CHCl_3$ and MCH systematically in mixtures by keeping the concentration of peptide **1** fixed at 0.05 mM (Fig. 2a). Peptide **1** exhibits UV-vis absorption in the range of 300–400 nm corresponding to the π–π* transition along the polarized long axis of the chromophore (NDI). In pure $CHCl_3$, two prominent peaks appeared at 361 nm and 382 nm with a shoulder at 342 nm. This corresponds to the characteristic NDI moiety in the non-aggregated monomeric state (Fig. 2a). After the addition of MCH to the $CHCl_3$ solution, a regular blue shift of these peaks was observed, followed by a decrease in the intensities of all these above mentioned peaks. At a 5 : 95 composition of $CHCl_3$: MCH, the 382 nm and 361 nm peaks shifted to 378 nm and 358 nm, respectively. Measuring and plotting the absorption maxima at a fixed wavelength (382 nm) against the % of MCH added reveals that after the composition of the $CHCl_3$: MCH mixture reaches 50 : 50, the aggregate starts to form considerably (Fig. 2b). Concentration dependent UV-vis spectroscopy (Fig. 2c) was performed at a 5 : 95 composition of

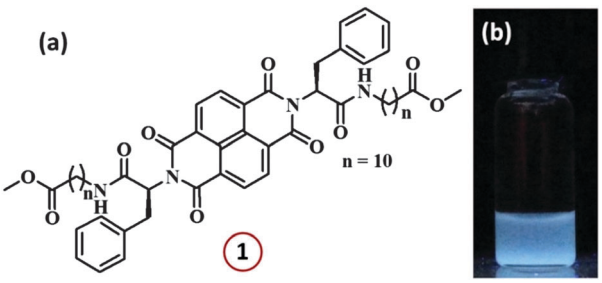

Fig. 1 (a) Chemical structure of peptide **1**. (b) Photograph of peptide **1** in a $CHCl_3$: MCH (10 : 90) solvent mixture under a UV lamp (365 nm) at 2 mM concentration.

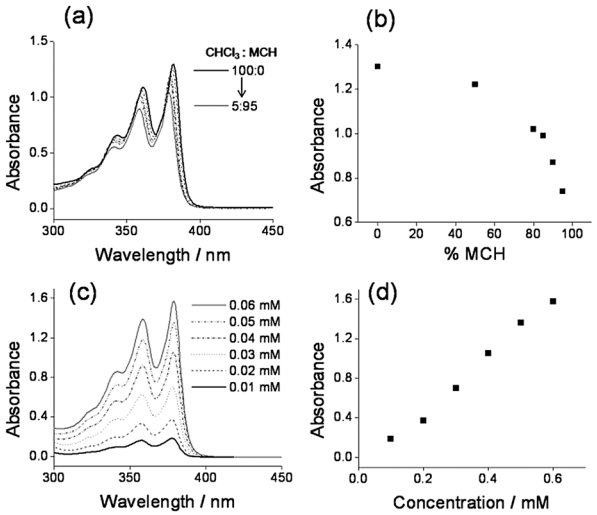

Fig. 2 The UV-vis study shows the (a) blue shift of the lowest energy absorption band indicating H-aggregation. (b) The absorbance *vs.* % of MCH plot shows a sharp decrease in absorbance with the increase in percentage of MCH (monitored at 382 nm). (c) The concentration dependent absorption plot and (d) the absorption *vs.* concentration plot shows a regular increase in absorbance with the increase in concentration (monitored at 378 nm). For (a and b) the concentration was 0.05 mM and for (c and d) the composition was 5 : 95 $CHCl_3$: MCH.

$CHCl_3$: MCH. The peaks appeared at similar positions (378 nm, 358 nm and 340 nm) and absorption was observed with a regular increase with an increase in the concentration of peptide **1** (Fig. 2d). The decrease in the intensity of these peaks ruled out solvatochromism. However, the decrease in intensity and the blue shift of the absorption band and the regular increase in intensity with an increase in concentration at a given solvent composition (5 : 95 composition of $CHCl_3$: MCH) clearly suggest the involvement of H-type stacking in the assembled state of the NDI chromophore.

From the monomeric state to aggregate formation, peptide **1** shows unusual emission properties corresponding to the formation of an H-aggregate. The solvent composition ($CHCl_3$: MCH) dependent fluorescence properties of peptide **1** were studied to investigate the aggregation induced fluorescence behavior (Fig. 3a). The addition of a nonpolar solvent like MCH in a solution of peptide **1** in $CHCl_3$ can significantly alter the aggregation pattern. From UV-vis spectroscopy, it is evident that at a higher percentage of MCH, peptide **1** forms an H-type aggregate. Peptide **1** at a 2 mM concentration in pure $CHCl_3$ shows a very weak fluorescence under UV lamp exposure (illuminated at 365 nm). The corresponding emission spectrum shows a peak at 410 nm (Fig. 3a). However, the addition of MCH (above 20 : 80 composition of $CHCl_3$: MCH) to the $CHCl_3$ solution of peptide **1**, keeping the concentration fixed at 2 mM, results in a bluish white color. This was observed from the aggregated solution under the exposure to a UV lamp illuminated at 365 nm. At a composition of 20 : 80 ($CHCl_3$: MCH), aggregation of peptide **1** was noticed and a broad emission band covering almost the entire visible spectral region was observed (Fig. 3a). With an increase in the percentage of MCH

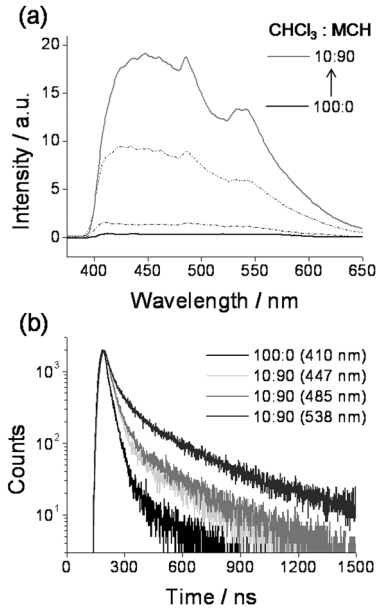

Fig. 3 (a) The fluorescence spectra of peptide **1** at different compositions of $CHCl_3$ and MCH at 2 mM concentration. (b) TCSPC decay profiles of peptide **1** in $CHCl_3$ (monitored = 410 nm) and the $CHCl_3$–MCH mixture (monitored = 447, 485 and 538 nm) at 0.2 mM concentration.

(>80%) the emission spectral intensity was remarkably enhanced with a broad band at around 447 nm followed by two shoulder peaks at 485 nm and at 538 nm. The broad unstructured emission band is a signature of excimer formation, as shown in non-peptide based derivatives of NDI and other dye molecules.[6,11] Generally in the H-aggregate quenching of fluorescence occurs due to rapid inter-band relaxation. However, it is also known that in the co-facial H-dimer arrangement of π-conjugated chromophores, a decrease in the inter-chromophoric distance occurs due to excitation.[11] This decrease in the inter-chromophoric distance leads to the formation of a low energy state that can be assigned as an excimer-like state. This excimer like state can result in weak long-lived fluorescence that is evident from the appearance of a broad fluorescence band.

To obtain more insights into the aggregation-induced change in emission properties, time-correlated single-photon-counting (TCSPC) experiments were performed (Fig. 3b and Table 1). For peptide **1** in $CHCl_3$, molecules were excited at 380 nm and emission was monitored at 410 nm. Short-lived decay was noted with an average lifetime of 828 ps, arising for the monomeric NDI dye owing to fast intersystem crossing to the close-lying triplet state.[12] Similar experiments were performed in $CHCl_3$: MCH (10 : 90) with excitation at 380 nm and the emission was monitored at 447, 485 and 538 nm. At 447 nm, bi-exponential decay was observed (Fig. 3b) with a substantially longer average lifetime of 1.26 ns. When the emission was monitored at 485 nm, a more long-lived species was traced with an average lifetime of 1.32 ns (Fig. 3b). When the emission was monitored at 538 nm an even longer average lifetime of 2.14 ns was found (Fig. 3b). The quantum yield was found to be 0.2%. These types of spectral features were reported by previous researchers with a comparable decay in the fluorescence lifetime that was observed for self-assembled NDI based organic nanoparticles.[6a] This is also attributed to excimer formation.

Table 1 TCSPC study of peptide **1**

Sample	N1	N2	τ_1 (ns)	τ_2 (ns)	τ (ns)	χ^2
Peptide **1** (410 nm)	0.1877	0.0029	0.764	4.907	0.828	1.014
Peptide **1** (447 nm)	2.5479	0.1068	0.995	7.272	1.26	1.002
Peptide **1** (485 nm)	2.9032	0.1610	0.997	7.185	1.32	1.006
Peptide **1** (538 nm)	0.0507	0.0083	1.220	7.755	2.14	1.126

Calculation of excimer properties[13] of the NDI aggregate is computationally intractable. Therefore, we have performed calculations on a model system for an NDI dimer [R = H] in which two NDI monomers are placed in a slipped-parallel (H-aggregate type) arrangement, similar to the experimentally obtained packing in the aggregate (Fig. S4, ESI†). Followed by this, the centre-to-centre distance between them is gradually increased from 3.3 Å to 6.0 Å at intervals of 0.25 Å. Well known DFT functionals such as B3LYP perform poorly for non-covalent interactions like π-stacking but the M06-2X functional was shown to give accurate geometries and energies for a variety of dispersion-dominated systems.[14] A shallow potential energy minimum is found for the dimer in the ground state reaction coordinate (Fig. 4a and b) which validates the dispersion correction in M06-2X. Then the vertical excitation energies for 10 excited states are calculated for each of the dimer geometries at various centre-to-centre distances obtained using TDDFT. Interestingly, an energy minimum is obtained in the first excited state when the centre-to-centre distance is 4.06 Å. It suggests the possibility of excimer formation at this geometry. According to gas-phase DFT modeling, the binding energy of two NDI monomers held by non-covalent interaction is −3.5 kcal mol^{-1}.

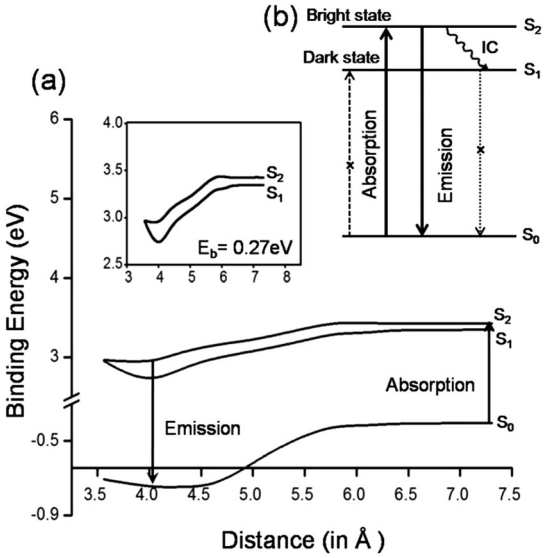

Fig. 4 (a) *Ab initio* potential energy surfaces of ground (S_0), first (S_1) and second excited (S_2) states as a function of inter-chromophore distance. Binding energy is shown as a function of distance between two NDI monomers units (E_b denotes the exciton binding energy). (b) Relaxation mechanism for excited states of the NDI dimer (IC = Internal Conversion).

The calculated exciton binding energy (E_b) as obtained from splitting between the S_1 and S_2 states (Fig. 4a and b) is 0.27 eV. This supports the possibility of NDI acting as an excellent optoelectronic material for OLEDs as the typical exciton binding energy for most organic materials is in the range of ~0.06–0.5 eV.[15] According to our TDDFT calculations, the strongly allowed (oscillator strength, $f = 0.26$) emission associated with the $S_2 \rightarrow S_0$ process involves transition from the LUMO to the HOMO−1 of the dimer (Fig. 5). Interestingly, the $S_1 \rightarrow S_0$ process is forbidden as is known for various H-aggregated aromatic molecules for which the lower state is dark while the higher lying state is bright.[16,8a] For this specific case, the $S_1 \rightarrow S_0$ transition composed of the LUMO → HOMO and the LUMO+1 → HOMO−1 is forbidden due to an even number of node differences between the virtual and filled orbitals. On the other hand, the LUMO → HOMO−1 orbitals which are involved in the $S_2 \rightarrow S_0$ transition are allowed due to the presence of one (odd) node difference between the virtual and filled orbitals (Fig. 5). The fact that this NDI dimer exhibits intense emission from the high lying excited state suggests that competing internal conversion IC ($S_2 \rightarrow S_1$) is a slow process and therefore, $k(S_2 \rightarrow S_0$, emission) > $k(S_2 \rightarrow S_1$, internal conversion). Violation of Kasha's rule was previously documented in the emission of oligothiophene encapsulated within a SWNT.[17] Recently, Brancato *et al.* have also reported fluorescence from coumarin dyes through Kasha's rule violation.[18] It is important to note that though a simple dimer splitting model[19] qualitatively explains the bright emission as observed experimentally, a more quantitative treatment shall require the relaxation of the nuclear coordinates of the excited states within implicit/explicit solvent which is avoided for the present work.

To obtain insights about the morphology of the aggregate field emission scanning electron microscopy (FE-SEM) and transmission electron microscopy (TEM) were performed. The FE-SEM image of the aggregate of peptide **1** showed entangled three dimensional fibrous networks (Fig. 6a) at 10 : 90 ($CHCl_3$: MCH) solvent composition. The widths of these fibers varied from 350 nm to 700 nm and they were several micrometers in length. Careful inspection of these fibers revealed that they were composed of numerous thin fibers of 90–150 nm in width. Interestingly, the TEM image (Fig. 6b) indicates that the aggregate is composed of very thin nanofibers and these nanofibers were 15–20 nm wide. The sample preparation for FE-SEM and TEM studies was different and that could be the reason for the difference in widths of these fibers.

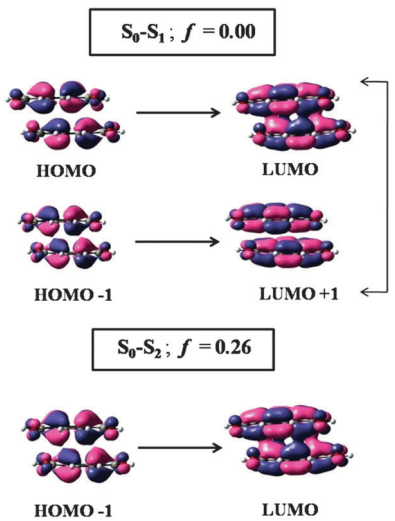

Fig. 5 Molecular orbitals involved in the optically allowed transition for the NDI dimer.

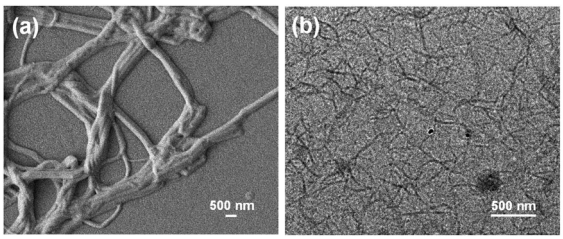

Fig. 6 (a) FE-SEM and (b) TEM images of the aggregated chromophore **1** in the $CHCl_3$–MCH mixture (10 : 90) show the entangled nanofiber network.

Experimental

NMR experiments

All NMR studies were carried out on a Bruker DPX500 MHz spectrometer at 300 K. Concentrations were in the range of 5–10 mmol in $CDCl_3$ or DMSO-d_6.

Mass spectrometry

Mass spectra were recorded on a Q-Tof microTM (Waters Corporation) mass spectrometer using the positive mode electrospray ionization process.

MALDI-TOF MS

MALDI-TOF MS analysis has been performed by using an Applied Biosystems MALDI TOF/TOF Analyzer in dithranol as a matrix.

Field emission scanning electron microscopic (FE-SEM) study

FE-SEM experiments were performed by placing a small portion of the sample (2 mM) on a microscope cover glass. Then, these samples were dried first in air and then in a vacuum and coated with platinum for 90 seconds at 10 kV voltages and 10 μA current. The average thickness of the coating layer of platinum was 3 to 4 nm. After that micrographs were taken by using a Jeol Scanning Microscope JSM-6700F.

Transmission electron microscopy (TEM) study

TEM images were recorded on a JEM 2010 electron microscope at an accelerating voltage of 200 kV. The solution of the compound was diluted (0.05 mM) and a drop of dilute solution was placed on carbon coated copper grids (300 mesh) and dried by slow evaporation. The grid was then allowed to dry in a vacuum for two days and then the image was taken.

UV/vis spectroscopy

UV/vis absorption spectra were recorded on a Hewlett-Packard (model 8453) UV/vis spectrophotometer (Varian Cary 50.bio).

PL spectroscopy

Fluorescence studies of the samples were carried out on a Perkin Elmer LS55 Fluorescence Spectrometer instrument. The sample was excited at a 340 nm wavelength and emission scans were recorded from 350 to 750 nm.

Time-correlated single photon counting (TCSPC) study

TCSPC measurements were performed using a Horiba Jobin Yvon IBH instrument having an MCP PMT Hamamatsu R3809 detector.

Quantum yield measurement

For compound **1** the quantum yield (Φ) has been calculated using Quinine Sulphate as a standard reference dye.[20]

Computational study

All calculations are performed using the M06-2X[21] hybrid DFT[22] functional with 6-31+G (d,p)[23] basis sets using Gaussian 09 software.[24] In order to study the excited state properties, we have used a time dependent density functional theory (TDDFT) based approach at the same level of theory.[25]

Conclusions

In summary, an NDI containing peptide based synthetic molecule **1** self-assembles to form H-aggregated species. However, in the H-aggregated state peptide **1** exhibits very unusual fluorescence behavior and this is in contrast to the commonly observed non-fluorescence properties of H-aggregated rylene dyes (NDIs, PBIs and others). Such unusual violation of Kasha's rule in the present case is validated through computational studies. A computational study vividly demonstrates that the transition probability from $S_2 \rightarrow S_0$ is more than that of $S_2 \rightarrow S_1$ and $S_1 \rightarrow S_0$ (dark state). The present study opens up the possibility of harnessing H-aggregated species for fluorescence related photonic applications of supramolecular materials.

Acknowledgements

S. B. N. N. and A. B. acknowledge CSIR and DST for financial assistance. AD thanks DST and INSA for partial funding. Computational resources of the IBM-P7 and CRAY supercomputer are duly acknowledged.

Notes and references

1 (*a*) S. S. Babu, V. K. Praveen and A. Ajayaghosh, *Chem. Rev.*, 2014, **114**, 1973; (*b*) A. Wilson, G. Gasparini and S. Matile, *Chem. Soc. Rev.*, 2014, **43**, 1948; (*c*) T-T-T. Nguyen, D. Türp, M. Wagner and K. Müllen, *Angew. Chem., Int. Ed.*, 2013, **52**, 669; (*d*) D. van der Zwaag, T. F. A. de Greef and E. W. Meijer, *Angew. Chem., Int. Ed.*, 2015, **54**, 8334; (*e*) L. Chen, K. S. Mali, S. R. Puniredd, M. Baumgarten, K. Parvez, W. Pisula, S. De Feyter and K. Müllen, *J. Am. Chem. Soc.*, 2013, **135**, 13531; (*f*) T. Yamamoto, T. Fukushima, A. Kosaka, W. Jin, Y. Yamamoto, N. Ishii and T. Aida, *Angew. Chem., Int. Ed.*, 2008, **47**, 1672; (*g*) C. Kulkarni and S. J. George, *Chem. – Eur. J.*, 2014, **20**, 4537; (*h*) D. K. Maiti and A. Banerjee, *Chem. Commun.*, 2013, **49**, 6909; (*i*) J. Baram, H. Weissman, Y. Tidhar, I. Pinkas and B. Rybtchinski, *Angew. Chem., Int. Ed.*, 2014, **53**, 4123; (*j*) D. K. Maiti and A. Banerjee, *Chem. – Asian J.*, 2013, **8**, 113; (*k*) S. S. Babu, V. K. Praveen, K. K. Kartha, S. Mahesh and A. Ajayaghosh, *Chem. – Asian J.*, 2014, **9**, 1830; (*l*) K. V. Rao, K. K. R. Datta, M. Eswaramoorthy and S. J. George, *Angew. Chem., Int. Ed.*, 2011, **50**, 1179; (*m*) S. Prasanthkumar, S. Ghosh, V. C. Nair, A. Saeki, S. Seki and A. Ajayaghosh, *Angew. Chem., Int. Ed.*, 2015, **54**, 946; (*n*) S. G. Ramkumar and S. Ramakrishnan, *Macromolecules*, 2010, **43**, 2307; (*o*) S. Bai, S. Debnath, N. Javid, P. W. J. M. Frederix, S. Fleming, C. Pappas and R. V. Ulijn, *Langmuir*, 2014, **30**, 7576; (*p*) M. A. J. Gillissen, M. M. E. Koenigs, J. J. H. Spiering, J. A. J. M. Vekemans, A. R. A. Palmans, I. K. Voets and E. W. Meijer, *J. Am. Chem. Soc.*, 2014, **136**, 336.

2 (*a*) R. Bhosale, J. Míšek, N. Sakai and S. Matile, *Chem. Soc. Rev.*, 2010, **39**, 138; (*b*) H. N. Tsao and K. Müllen, *Chem. Soc. Rev.*, 2010, **39**, 2372; (*c*) A. L. Sisson, N. Sakai, N. Banerji, A. Fürstenberg, E. Vauthey and S. Matile, *Angew. Chem., Int. Ed.*, 2008, **47**, 3727; (*d*) S. Prasanthkumar, A. Gopal and A. Ajayaghosh, *J. Am. Chem. Soc.*, 2010, **132**, 13206; (*e*) S. Roy, D. K. Maiti, S. Panigrahi, D. Basak and A. Banerjee, *Phys. Chem. Chem. Phys.*, 2014, **16**, 6041; (*f*) A. Coskun, J. M. Spruell, G. Barin, W. R. Dichtel, A. H. Flood, Y. Y. Botros and J. F. Stoddart, *Chem. Soc. Rev.*, 2012, **41**, 4827.

3 (*a*) S. K. M. Nalluri, C. Berdugo, N. Javid, P. W. J. M. Frederix and R. V. Ulijn, *Angew. Chem., Int. Ed.*, 2014, **53**, 5882; (*b*) M. B. Avinash and T. Govindaraju, *Adv. Funct. Mater.*, 2011, **21**, 3875; (*c*) F. B. L. Cougnon, N. Ponnuswamy, N. A. Jenkins, G. D. Pantoş and J. K. M. Sanders, *J. Am. Chem. Soc.*, 2012, **134**, 19129; (*d*) F. B. L. Cougnon, H. Y. A-Yeung, G. D. Pantoş and J. K. M. Sanders, *J. Am. Chem. Soc.*, 2011, **133**, 3198; (*e*) H. Shao, J. Seifert, N. C. Romano, M. Gao, J. J. Helmus, C. P. Jaroniec, D. A. Modarelli and J. R. Parquette, *Angew. Chem., Int. Ed.*, 2010, **49**, 7688; (*f*) H. Shao and J. R. Parquette, *Chem. Commun.*, 2010, **46**, 4285; (*g*) E. R. Draper, J. J. Walsh, T. O. McDonald, M. A. Zwijnenburg, P. J. Cameron, A. J. Cowan and D. J. Adams, *J. Mater. Chem. C*, 2014, **2**, 5570; (*h*) B. D. Wall, A. E. Zacca, A. M. Sanders, W. L. Wilson, A. L. Ferguson and J. D. Tovar, *Langmuir*, 2014, **30**, 5946.

4 (*a*) P. Mukhopadhyay, Y. Iwashita, M. Shirakawa, S.-i. Kawano, N. Fujita and S. Shinkai, *Angew. Chem., Int. Ed.*, 2006, **45**, 1592; (*b*) S. Basak, S. Bhattacharya, A. Datta and A. Banerjee, *Chem. – Eur. J.*, 2014, **20**, 5721; (*c*) Y. Zhao, C. Beuchat, Y. Domoto, J. Gajewy, A. Wilson, J. Mareda, N. Sakai and S. Matile, *J. Am. Chem. Soc.*, 2014, **136**, 2101;

(*d*) S. De and S. Ramakrishnan, *Chem. – Asian J.*, 2011, **6**, 149; (*e*) G. M. Prentice, S. I. Pascu, S. V. Filip, K. R. West and G. Dan Pantoş, *Chem. Commun.*, 2015, **51**, 8265.

5 S. V. Bhosale, C. H. Jani and S. J. Langford, *Chem. Soc. Rev.*, 2008, **37**, 331.

6 (*a*) M. Kumar and S. J. George, *Nanoscale*, 2011, **3**, 2130; (*b*) T. D. M. Bell, S. V. Bhosale, C. M. Forsyth, D. Hayne, K. P. Ghiggino, J. A. Hutchison, C. H. Jani, S. J. Langford, M. A.-P. Lee and C. P. Woodward, *Chem. Commun.*, 2010, **46**, 4881; (*c*) S. Basak, J. Nanda and A. Banerjee, *Chem. Commun.*, 2013, **49**, 6891; (*d*) S. Basak, N. Nandi and A. Banerjee, *Chem. Commun.*, 2015, **51**, 780.

7 F. Würthner, S. Ahmed, C. Thalacker and T. Debaerdemaeker, *Chem. – Eur. J.*, 2002, **8**, 4742.

8 (*a*) F. Würthner, T. E. Kaiser and C. R. S-Möller, *Angew. Chem., Int. Ed.*, 2011, **50**, 3376; (*b*) S. Ghosh, X.-Q. Li, V. Stepanenko and F. Würthner, *Chem. – Eur. J.*, 2008, **14**, 11343.

9 (*a*) T. E. Kaiser, V. Stepanenko and F. Würthner, *J. Am. Chem. Soc.*, 2009, **131**, 6719; (*b*) T. E. Kaiser, H. Wang, V. Stepanenko and F. Würthner, *Angew. Chem., Int. Ed.*, 2007, **46**, 5541.

10 (*a*) N. J. Turro, *Modern Molecular Photochemistry*, Benjamin/Cummings Pub. Inc., California, 1978; (*b*) A. S. Davydov, *Theory of Molecular Excitons*, Springer Sci, NY, 1971.

11 (*a*) U. Rösch, S. Yao, R. Wortmann and F. Würthner, *Angew. Chem., Int. Ed.*, 2006, **45**, 7026; (*b*) M. Kumar and S. J. George, *Chem. – Eur. J.*, 2011, **17**, 11102; (*c*) N. S. S. Kumar, S. Varghese, C. H. Suresh, N. P. Rath and S. Das, *J. Phys. Chem. C*, 2009, **113**, 11927.

12 T. C. Barros, S. Brochsztain, V. G. Toscano, P. B. Filho and M. J. Politi, *J. Photochem. Photobiol., A*, 1997, **111**, 97.

13 H. Saigusa and E. C. Lim, *Acc. Chem. Res.*, 1996, **29**, 171.

14 (*a*) A. K. Jissy and A. Datta, *J. Phys. Chem. B*, 2013, **117**, 8340; (*b*) A. K. Jissy and A. Datta, *J. Phys. Chem. Lett.*, 2013, **4**, 1018.

15 (*a*) D. Moses, J. Wang, A. J. Heeger, N. Kirova and S. Brazovski, *Proc. Natl. Acad. Sci. U. S. A.*, 2001, **98**, 13496; (*b*) M. Knupfer, *Appl. Phys. A: Mater. Sci. Process.*, 2003, **77**, 623.

16 P. J. Vallett, J. L. Snyder and N. H. Damrauer, *J. Phys. Chem. A*, 2013, **117**, 10824.

17 K. Yanagi and H. Kataura, *Nat. Photonics*, 2010, **4**, 200.

18 G. Brancato, G. Signore, P. Neyroz, D. Polli, G. Cerullo, G. Abbandonato, L. Nucara, V. Barone, F. Beltram and R. Bizzarri, *J. Phys. Chem. B*, 2015, **119**, 6144.

19 (*a*) A. Datta and S. K. Pati, *J. Chem. Phys.*, 2003, **118**, 8420; (*b*) A. Datta and S. K. Pati, *Chem. Soc. Rev.*, 2006, **35**, 1305.

20 A. T. R. Williams, S. A. Winfield and J. N. Miller, *Analyst*, 1983, **108**, 1067.

21 Y. Zhao and D. G. Truhlar, *Theor. Chem. Acc.*, 2008, **120**, 215.

22 W. Kohn and L. J. Sham, *Phys. Rev. A: At., Mol., Opt. Phys.*, 1965, **140**, 1133.

23 W. J. Hehre, R. Ditchfield and J. A. Pople, *J. Chem. Phys.*, 1972, **56**, 2257.

24 M. J. Frisch, G. W. Trucks, H. B. Schlegel, G. E. Scuseria, M. A. Robb, J. R. Cheeseman, G. Scalmani, V. Barone, B. Mennucci, G. A. Petersson, H. Nakatsuji, M. Caricato, X. Li, H. P. Hratchian, A. F. Izmaylov, J. Bloino, G. Zheng, J. L. Sonnenberg, M. Hada, M. Ehara, K. Toyota, R. Fukuda, J. Hasegawa, M. Ishida, T. Nakajima, Y. Honda, O. Kitao, H. Nakai, T. Vreven, J. A. Jr. Montgomery, J. E. Peralta, F. Ogliaro, M. Bearpark, J. J. Heyd, E. Brothers, K. N. Kudin, V. N. Staroverov, R. Kobayashi, J. Normand, K. Raghavachari, A. Rendell, J. C. Burant, S. S. Iyengar, J. Tomasi, M. Cossi, N. Rega, N. J. Millam, M. Klene, J. E. Knox, J. B. Cross, V. Bakken, C. Adamo, J. Jaramillo, R. Gomperts, R. E. Stratmann, O. Yazyev, A. J. Austin, R. Cammi, C. Pomelli, J. W. Ochterski, R. L. Martin, K. Morokuma, V. G. Zakrzewski, G. A. Voth, P. Salvador, J. J. Dannenberg, S. Dapprich, A. D. Daniels, Ö. Farkas, J. B. Foresman, J. V. Ortiz, J. Cioslowski and D. J. Fox, *Gaussian 09*, Gaussian, Inc., Wallingford CT, 2009.

25 J. C. Amicangelo, *J. Phys. Chem. A*, 2005, **109**, 9174.

